Electronic supplementary information (ESI)

Luminescence property modulation through structural modification of coordination polymers for ratiometric detection of mercuric ions in aqueous media

Rakesh Kumar[a], Anupam Maiti[a], Bidyadhar Mahato[a] and Debajyoti Ghoshal[a]*

[a] Department of Chemistry, Jadavpur University, Jadavpur, Kolkata, 700032, India

E-mail: debajyoti.ghoshal@jadavpuruniversity.in

Table S1. Crystallographic data and structural refinement parameters for compound **1**, **2** and **3**

	1	**2**	**3**
Formula	$C_{40}H_{32}MnN_{10}O_7$	$C_{40}H_{31}CoN_{10}O_{6.5}$	$C_{44}H_{36}MnN_6O_7$
Formula Weight	819.70	814.68	815.73
Crystal System	Triclinic	Triclinic	Triclinic
Space group	*P-1*	*P-1*	*P-1*
a/ Å	7.4180(4)	7.4337(2)	7.5222(3)
b/Å	10.4640(5)	10.3464(3)	10.5057(5)
c/ Å	13.3907(6)	13.1723(4)	13.4534(6)
α/°	107.421(1)	107.531(1)	105.481(1)
β/°	103.868(1)	103.410(1)	104.538(1)
γ/°	94.011(2)	92.959(1)	93.879(1)
V/ Å3	951.49(8)	931.62(5)	981.40(8)
Z	1	1	1
D_c/ g cm^{-3}	1.431	1.452	1.380
μ /mm^{-1}	0.412	0.526	0.397
F(000)	423	420	423
θ range/°	2.9-27.6	3.3-27.6	2-27.6
Reflections collected	33955	33183	31823
Unique reflections	4377	4296	4497
Reflections $I > 2\sigma(I)$	4009	3861	3885
R_{int}	0.046	0.062	0.074
goodness-of-fit (F^2)	1.09	1.10	1.26
R_1 ($I > 2\sigma(I)$) [a]	0.0392	0.0392	0.0698
$wR_2(I > 2\sigma(I))$ [a]	0.1113	0.0907	0.1318

[a] $R_1 = \Sigma \left| \left| F_o \right| - \left| F_c \right| \right| / \Sigma \left| F_o \right|$, $wR_2 = [\Sigma (w (F_o^2 - F_c^2)^2) / \Sigma w (F_o^2)^2]^{1/2}$

Table S2. Selected Bond Lengths (Å) and Bond Angles (°) for **1**.

Mn1-O1	2.1528(13)	Mn1-O1W	2.1755(15)
Mn1-N1	2.3331(15)	Mn1-O1^a	2.1528(13)
Mn1-O1W^a	2.1755(15)	Mn1-N1^a	2.3331(15)
O1-Mn1-O1W	90.16(5)	O1-Mn1-N1	95.22(5)
O1-Mn1-O1^a	180.00	O1-Mn1-O1W^a	89.84(5)
O1-Mn1-N1^a	84.78(5)	O1W-Mn1-N1	88.41(5)
O1W-Mn1-O1^a	89.84(5)	O1W-Mn1-O1W^a	180.00
O1W-Mn1-N1^a	91.59(5)	N1-Mn1-O1^a	84.78(5)
N1-Mn1-O1W^a	91.59(5)	N1-Mn1-N1^a	180.00
O1^a-Mn1-O1W^a	90.16(5)	O1^a-Mn1-N1^a	95.22(5)
O1W^a-Mn1-N1^a	88.41(5)		

a = -x, 2-y,1-z

Table S3. Selected Bond Lengths (Å) and Bond Angles (°) for **2**.

Co1-O1	2.0926(13)	Co1-O1W	2.0871(16)
Co1-N1	2.1989(15)	Co1-O1^{a}	2.0926(13)
Co1-O1W^{a}	2.0871(16)	Co1-N1^{a}	2.1989(15)
O1-Co1-O1W	89.75(6)	O1-Co1-N1	85.58(5)
O1-Co1-O1^{a}	180.00	O1-Co1-O1W^{a}	90.25(6)
O1-Co1-N1^{a}	94.42(5)	O1W-Co1-N1	87.94(6)
O1W-Co1-O1^{a}	90.25(6)	O1W-Co1-O1W^{a}	180.00
O1W-Co1-N1^{a}	92.06(6)	N1-Co1-O1^{a}	94.42(5)
N1-Co1-O1W^{a}	92.06(6)	N1-Co1-N1^{a}	180.00
O1^{a} -Co1-O1W^{a}	89.75(6)	O1^{a} -Co1-N1^{a}	85.58(5)
O1W^{a}-Co1-N1^{a}	87.94(6)		

a = 2-x,1-y,2-z

Table S4. Selected Bond Lengths (Å) and Bond Angles (°) for **3**.

Mn1-O1	2.156(2)	Mn1-O1W	2.183(2)
Mn1-N1	2.316(3)	Mn1-O1^{a}	2.156(2)
Mn1-O1W^{a}	2.183(2)	Mn1 -N1^{a}	2.316(3)
O1 -Mn1-O1W	89.36(9)	O1-Mn1-N1	85.49(8)
O1-Mn1-O1^{a}	180.00	O1-Mn1-O1W^{a}	90.64(9)
O1 -Mn1-N1^{a}	94.52(8)	O1W-Mn1-N1	88.66(9)
O1W- Mn1-O1^{a}	90.64(9)	O1W-Mn1-O1W^{a}	180.00
O1W-Mn1-N1^{a}	91.34(9)	N1-Mn1-O1^{a}	94.52(8)
N1-Mn1-O1W ^{a}	91.34(9)	N1-Mn1-N1 ^{a}	180.00
O1^{a} -Mn1-O1W ^{a}	89.36(9)	O1^{a} -Mn1-N1 ^{a}	85.49(8)
O1W^{a} -Mn1-N1 ^{a}	88.66(9)		

a = -x,1-y,-z

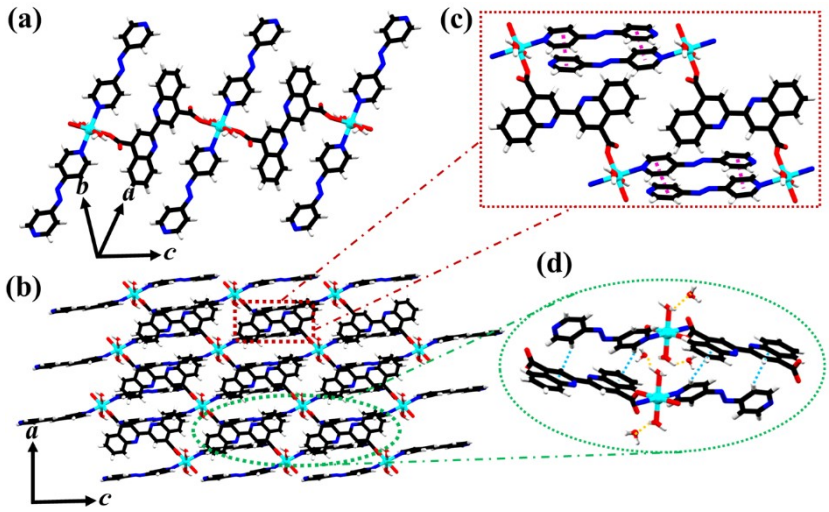

Fig. S1 (a) Diagram of 1D chain of compound **2** constructed through metal (Co) and dicarboxylyate (bqdc) along the diagonal of *ac* plane. (b) Overall 3D representation of **2**. (c) View of supramolecular intermolecular π···π interaction along the *b* axis (magenta dotted line). (d) View of supramolecular C-H···π interaction (cyan dotted line) and intermolecular hydrogen bonding interaction (orange dotted line) along the *b* axis.

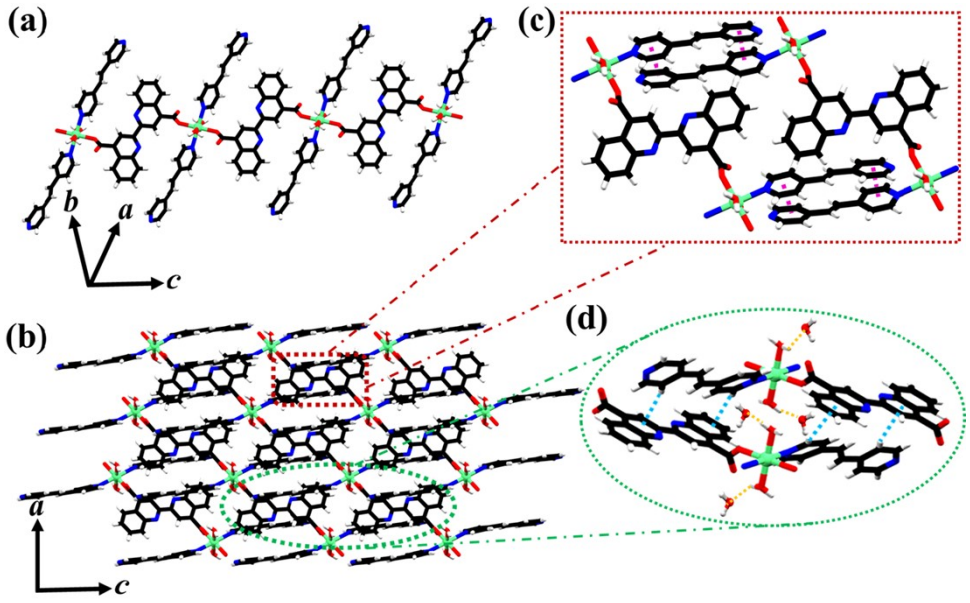

Fig. S2 (a) Diagram of 1D chain of compound **3** constructed through metal (Mn) and dicarboxylyate (bqdc) along the diagonal of *ac* plane. (b) Overall 3D representation of **3**. (c) View of supramolecular intermolecular π···π interaction along the *b* axis (magenta dotted line). (d) View of supramolecular C-H···π interaction (cyan dotted line) and intermolecular hydrogen bonding interaction (orange dotted line) along the *b* axis.

Table S5. π-π interactions for compound **1**

Ring (i)→ring (j)	distance of centroid (i) from ring (j), (Å)	dihedral angle (i,j) (deg)	distance between the (i,j) ring centroids, (Å)
R(1)→R(2)^{I}	3.8674(12)	10.27(10)	3.2956(8)
R(2)→R(1)^{I}	3.8675(12)	10.27(10)	3.5949(8)
R(2)→R(2)^{J}	4.3221(11)	0.020(9)	3.3095(8)

Symmetry code: I = -X, 1-Y, -Z; J= 1-X, 1-Y, -Z

R(i)/R(j) denotes the rings in the corresponding structures:

R(1) = N1/C1/C3/C5/C4/C2.

R(2)= N4/C9/C7/C6/C8/C10.

Table S6. C-H…π interactions for **1**

C-H ring(j)	H...R distance (Å)	C-H...R angle (deg)	C...R distance (Å)
C1 -H1→R(4)^{J}	2.97	134	3.682(2)
C3 -H3→R(3)^{J}	2.81	129	3.476(2)

Symmetry code: J=1-X, 2-Y, 1-Z

R(j) denotes the rings in the corresponding structures:

R(3) = N5/C14/C13/C12/C15/C16.

R(4) = C15/C16/C17/C18/C19/C20.

Table S7. Hydrogen bonding interactions for compound **1**

D–H···A	D–H	H···A	D···A	D–H···A
O2W—H2WA..O2	0.85	1.90	2.661(6)	148
O2W—H2WB..O2	0.85	1.80	2.624(6)	162
O1W--H1WA..N4	0.870(14)	1.937(13)	2.777(2)	162(2)
O1W--H1WB..O2W	0.87(3)	2.42(2)	3.121(6)	138(2)

Table S8. π-π interactions for **2**

Ring (i)→ring (j)	distance of centroid (i) from ring (j), (Å)	dihedral angle (i,j) (deg)	distance between the (i,j) ring centroids, (Å)
R(1)→R(2)^{I}	3.8775(12)	11.27(10)	3.2921(9)
R(2)→R(1)^{I}	3.8775(12)	11.27(10)	3.6084(9)
R(2)→R(2)^{J}	4.3967(11)	0.00(10)	3.2992(9)

Symmetry code: I = 2-X,-Y,1-Z; J= 3-X,-Y,1-Z

R(i)/R(j) denotes the rings in the corresponding structures:

R(1) = N1/C1/C2/C3/C4/C5.

R(2)= N4/C8/C7/C6/C10/C9.

Table S9. C-H…π interactions for **2**

C-H ring(j)	H...R distance (Å)	C-H...R angle (deg)	C...R distance (Å)
C4 -H4→R(3)^{K}	2.86	126	3.490(2)
C5 -H5→R(4)^{K}	2.97	132	3.661(2)
C10 -H10→R(3)^{L}	2.97(3)	136.8(18)	3.696(2)

Symmetry code: K= 1+X,Y,Z; L= 2-X,1-Y,1-Z

R(j) denotes the rings in the corresponding structures:

R(3)= N5/C14/C15/C12/C13/C20.

R(4)= C14/C15/C16/C17/C18/C19.

Table S10. Hydrogen bonding interactions for compound **2**

D–H···A	D–H	H···A	D···A	D–H···A
O1W--H1WA..N4	0.80(3)	2.00(2)	2.777(2)	166(3)
O1W--H1WB..O2W	0.92(4)	2.48(4)	3.15(2)	130(3)

Table S11. π-π interactions for **3**

Ring (i)→ring (j)	distance of centroid (i) from ring (j), (Å)	dihedral angle (i,j) (deg)	distance between the (i,j) ring centroids, (Å)
R(1)→R(2)^{I}	3.9274(19)	13.42(16)	3.2474(14)
R(2)→R(1)^{I}	3.9274(19)	13.42(16)	3.6507(13)
R(2)→R(2)^{J}	4.5610(15)	0.00(16)	3.3424(13)

Symmetry code: I = -X,2-Y,1-Z; J= -1-X, 2-Y, 1-Z

R(j) denotes the rings in the corresponding structures:

R(1) = N1/C1/C5/C4/C3/C2.

R(2)= N4/C9/C8/C6/C7/C10.

Table S12. C-H…π interactions for **3**

C-H ring(j)	H...R distance (Å)	C-H...R angle (deg)	C...R distance (Å)
C1-H1→R(4)^{K}	2.99	133	3.678(4)
C5-H5→R(3)^{K}	2.82	132	3.510(4)
C7-H7→R(3)^{L}	2.99	143	3.769(4)

Symmetry code: K= -1+X, Y, Z; L=-X, 1-Y, 1-Z

R(j) denotes the rings in the corresponding structures:

R(3)= N5/C18/C13/C12/C19/C20.

R(4)= C13/C14/C15/C16/C17/C18.

Table S13. Hydrogen bonding interactions for **3**

D–H···A	D–H	H···A	D···A	D–H···A
O2W--H2WA..O2	0.85	1.97	2.674(10)	139
O2W--H2WB..O2	0.85	1.86	2.630(9)	151
O1W--H1WB..O2W	0.88(5)	2.56(5)	3.221(10)	132(4)'

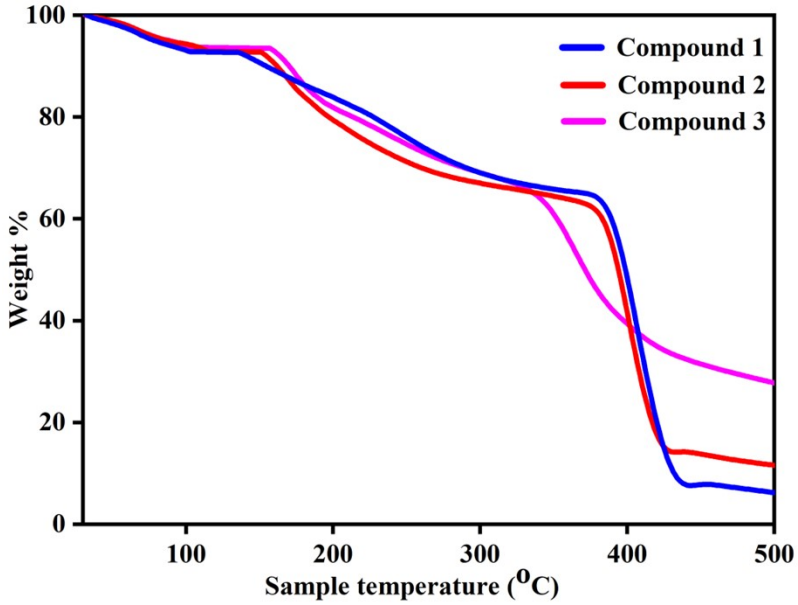

Fig. S3 TGA curves for compounds **1**–**3**

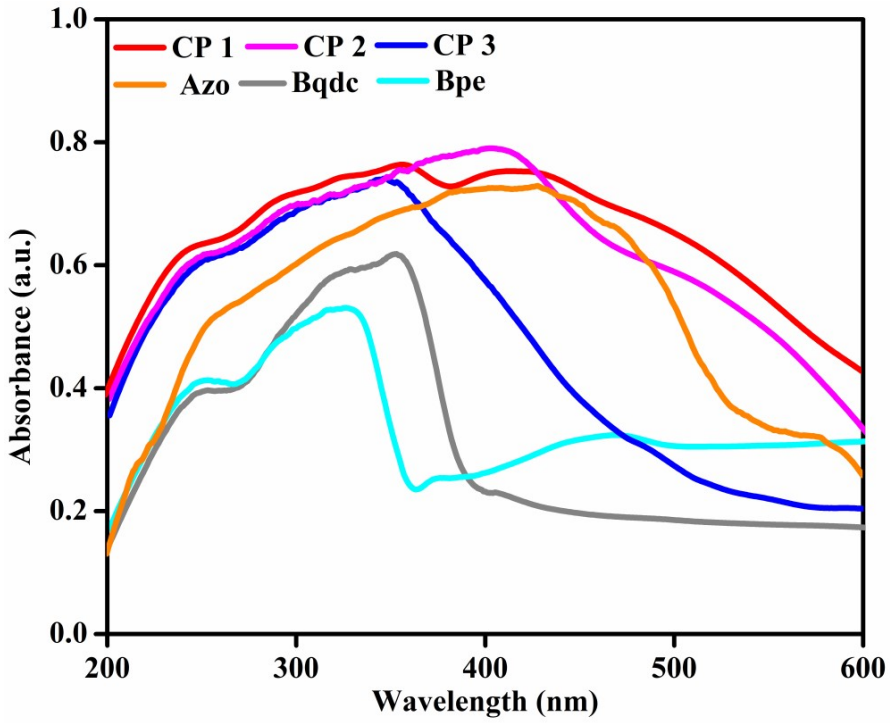

Fig. S4 UV- vis spectrum of all compounds **1**–**3** with all the ligand used for these CPs syntheses

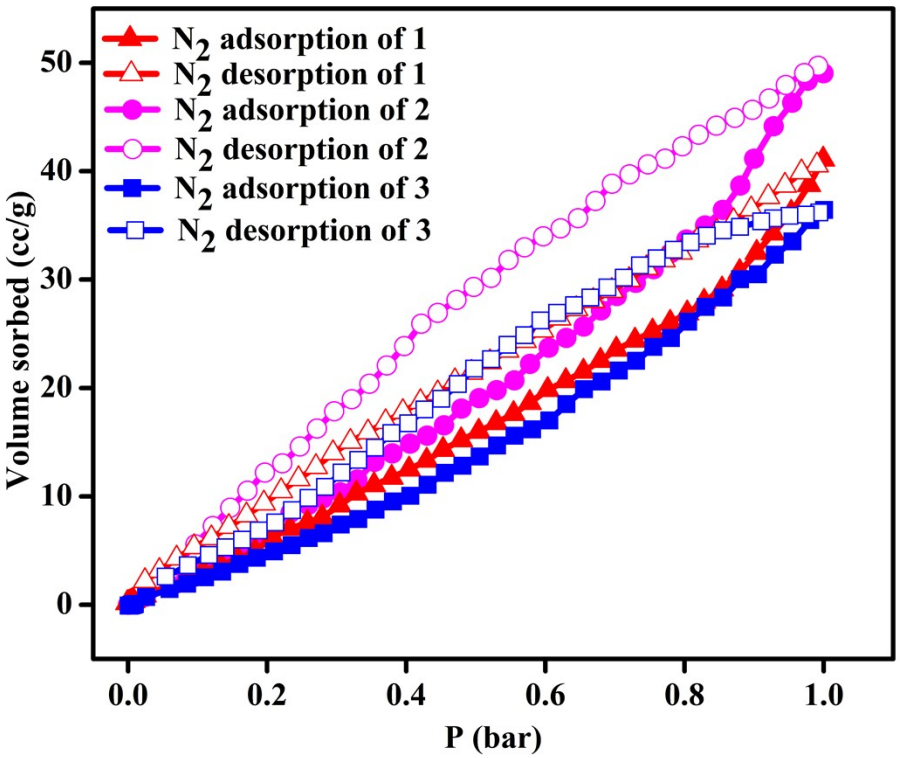

Fig. S5 N_2 adsorption isotherm curve of compound **1** (red), **2** (magenta) and **3** (blue) at 77 K and 1 bar. Filled and open symbol denote the adsorption and desorption respectively.

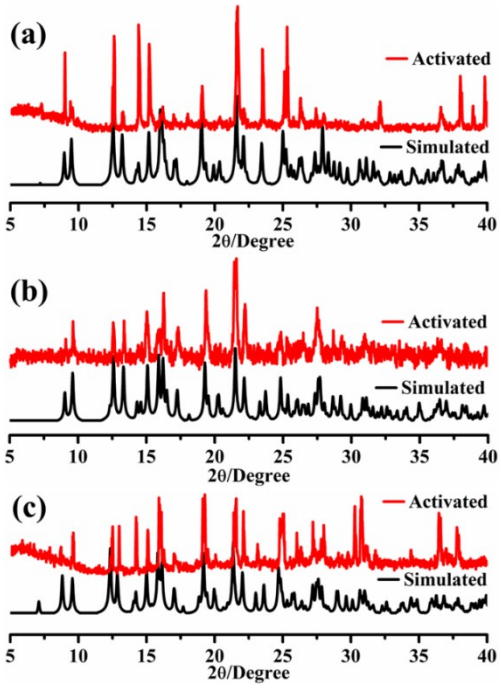

Fig. S6 PXRD peak pattern of all the compounds after N_2 sorption study.

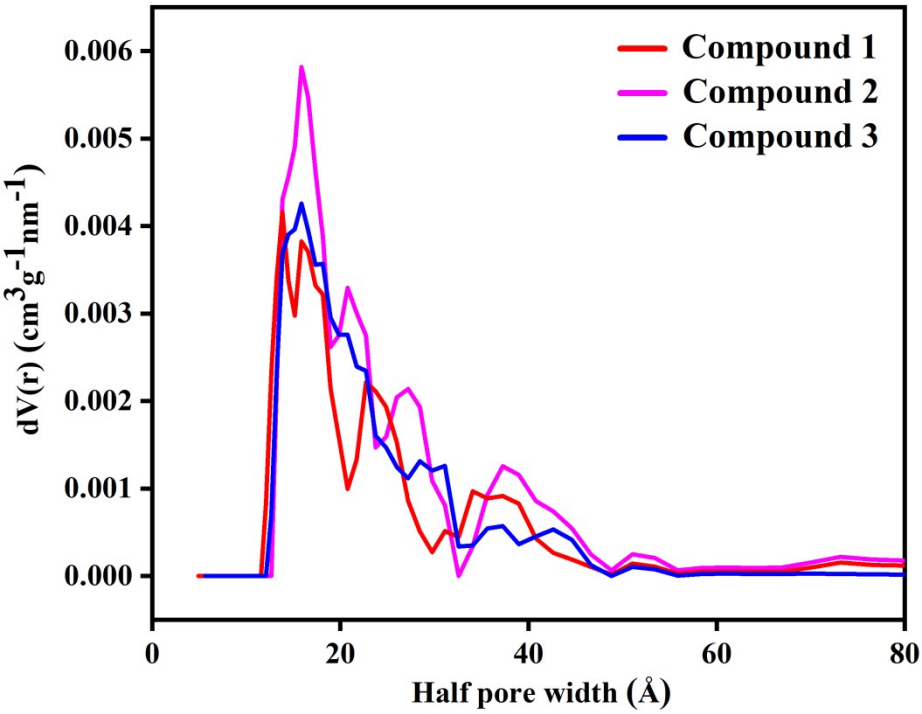

Fig. S7 Pore size distribution plot for all three compounds

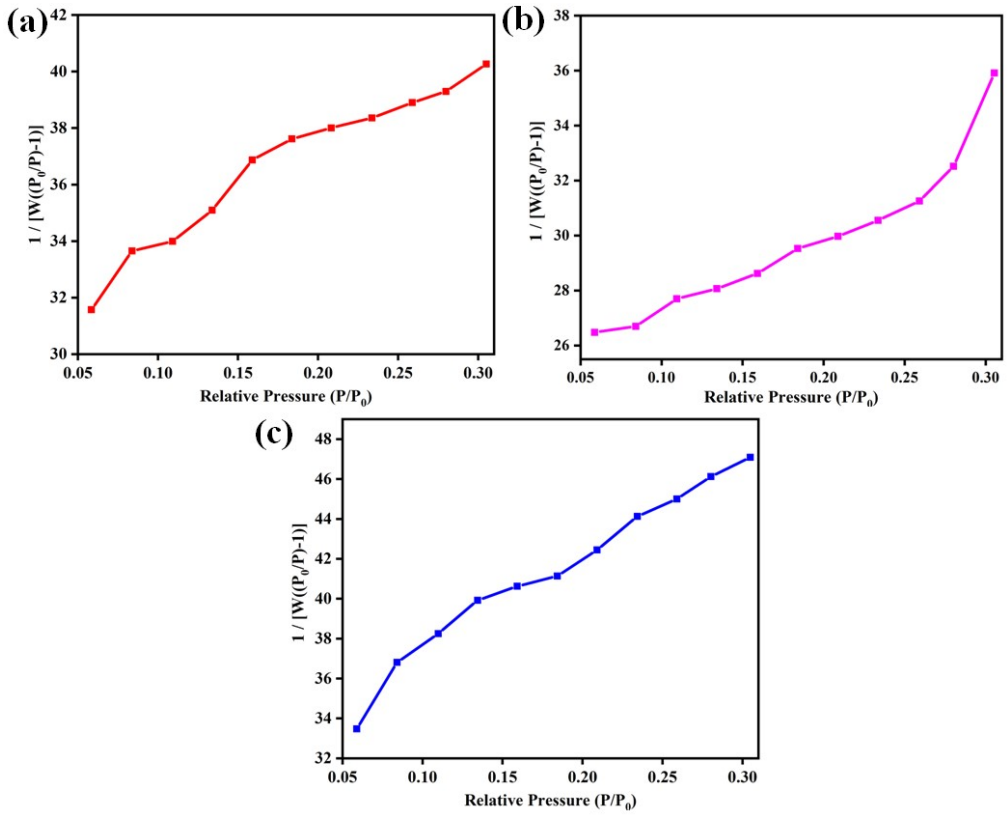

Fig. S8 Typical BET plot for (a) **1** (b) **2** and (c) **3**, used to determine the surface area of all three materials based on N_2 adsorption data at 77 K. It is represented by a plot of 1 / [$W(P_0/P) - 1$] versus P/P_0. The linearity observed within the relative pressure range of 0.05 to 0.30 confirms the applicability of the BET theory for these materials

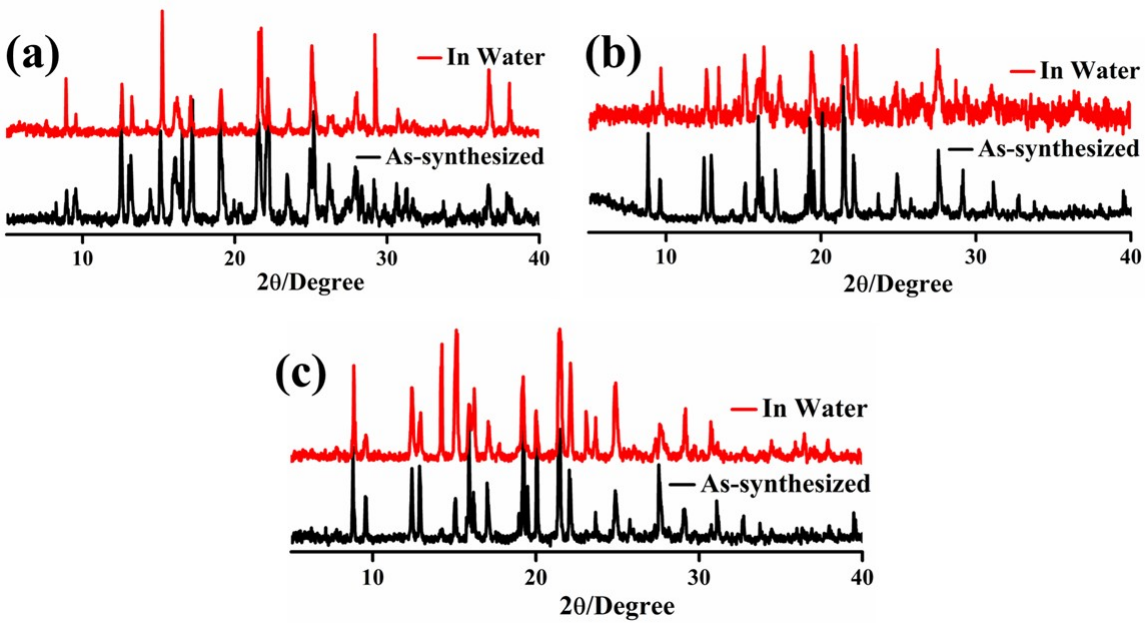

Fig. S9 PXRD pattern of compound (a) **1;** (b) **2** and (c) **3** after 1 week water treatment

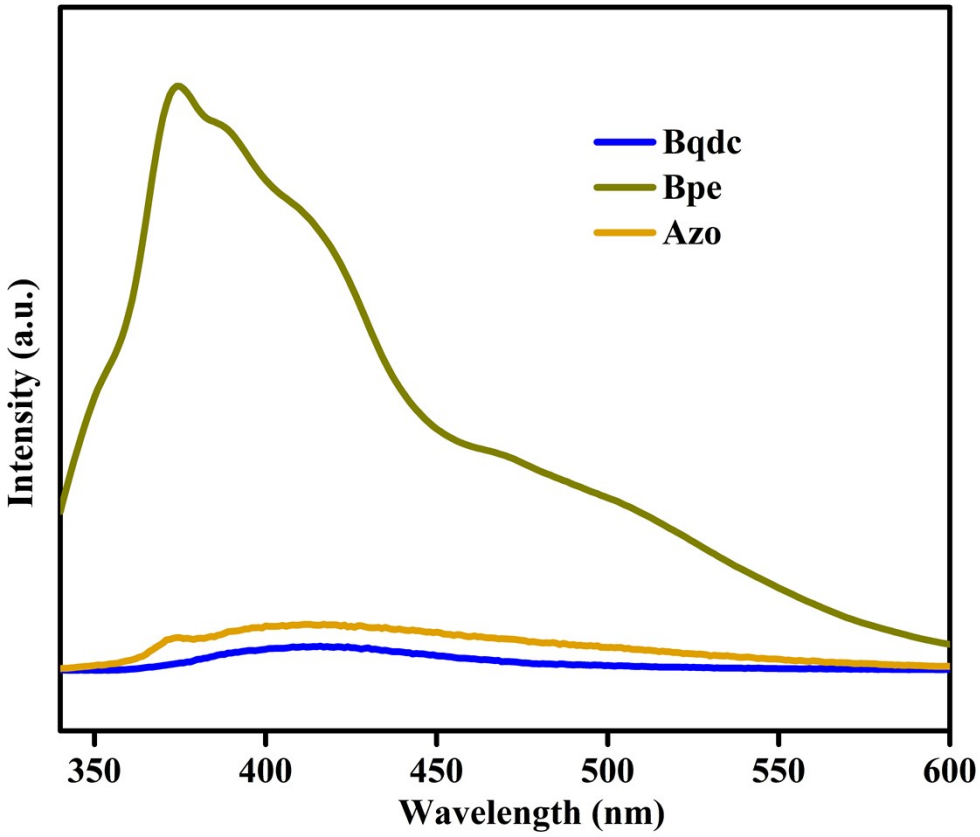

Fig. S10 Emission spectra of ligands used for CPs constriction

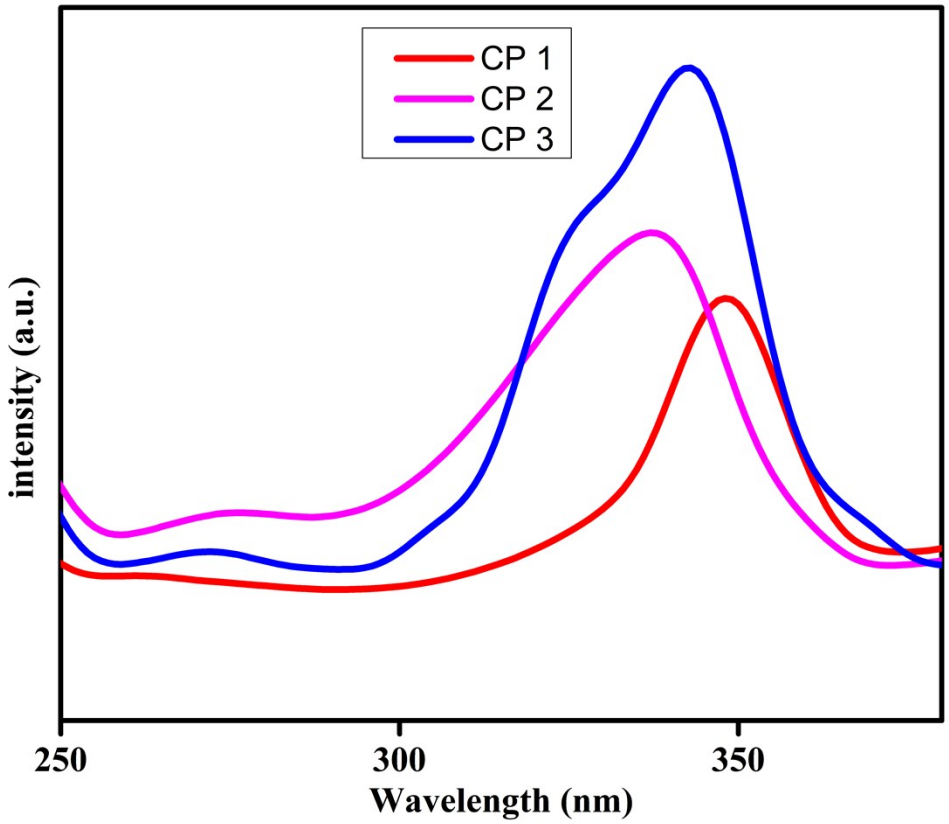

Fig. S11 Excitation spectra of compound **1-3**.

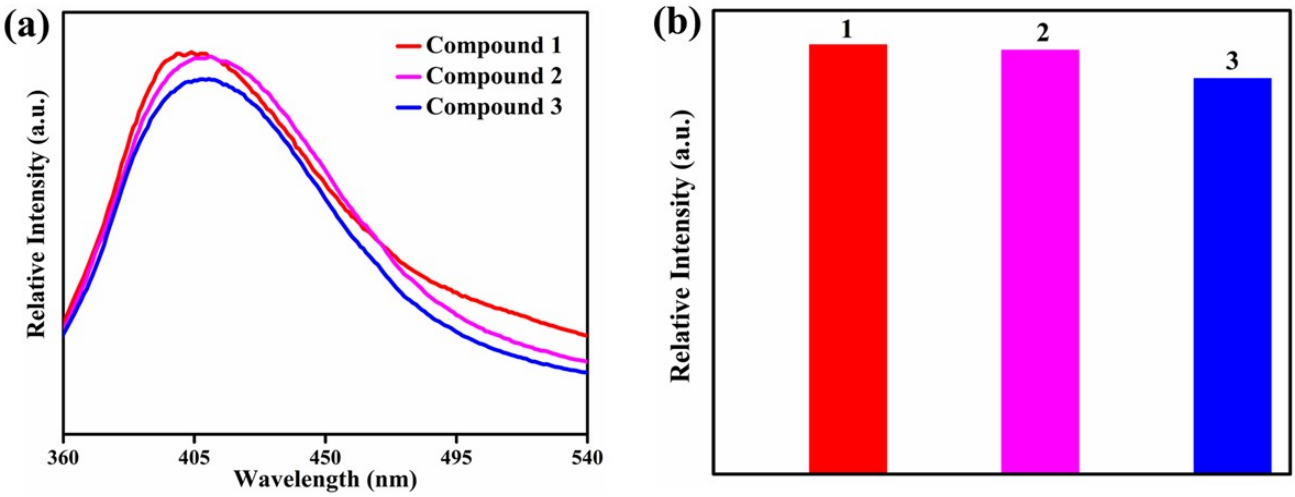

Fig. S12 (a) emission spectra and (b) bar diagram comparing relative intensity for emission of compound **1-3**.

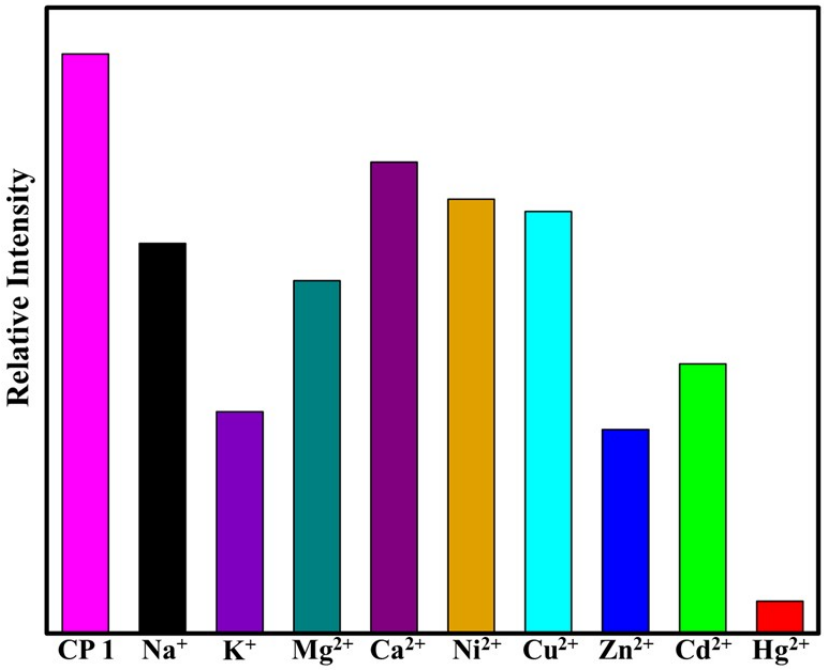

Fig. S13 Bar graph illustrating the emission response of compound **1** in the presence of various metal ions

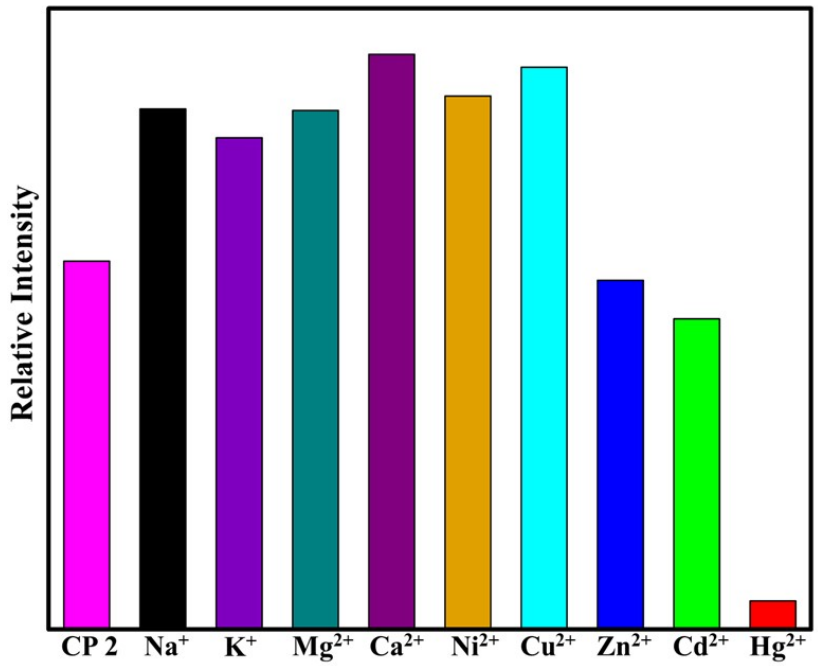

Fig. S14 Bar graph illustrating the emission response of compound **2** in the presence of various metal ions

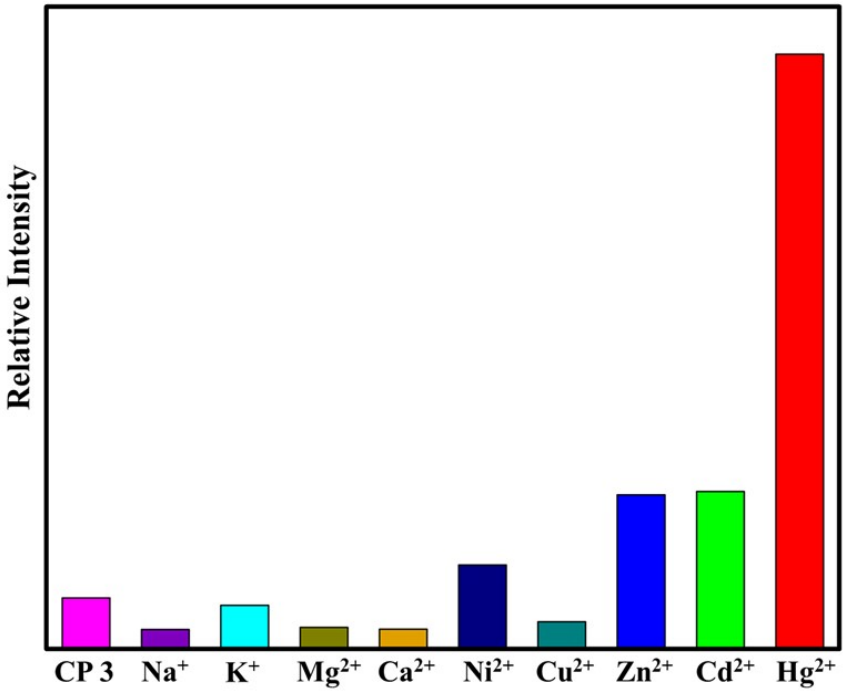

Fig. S15 Bar graph illustrating the emission response of compound **3** in the presence of various metal ions

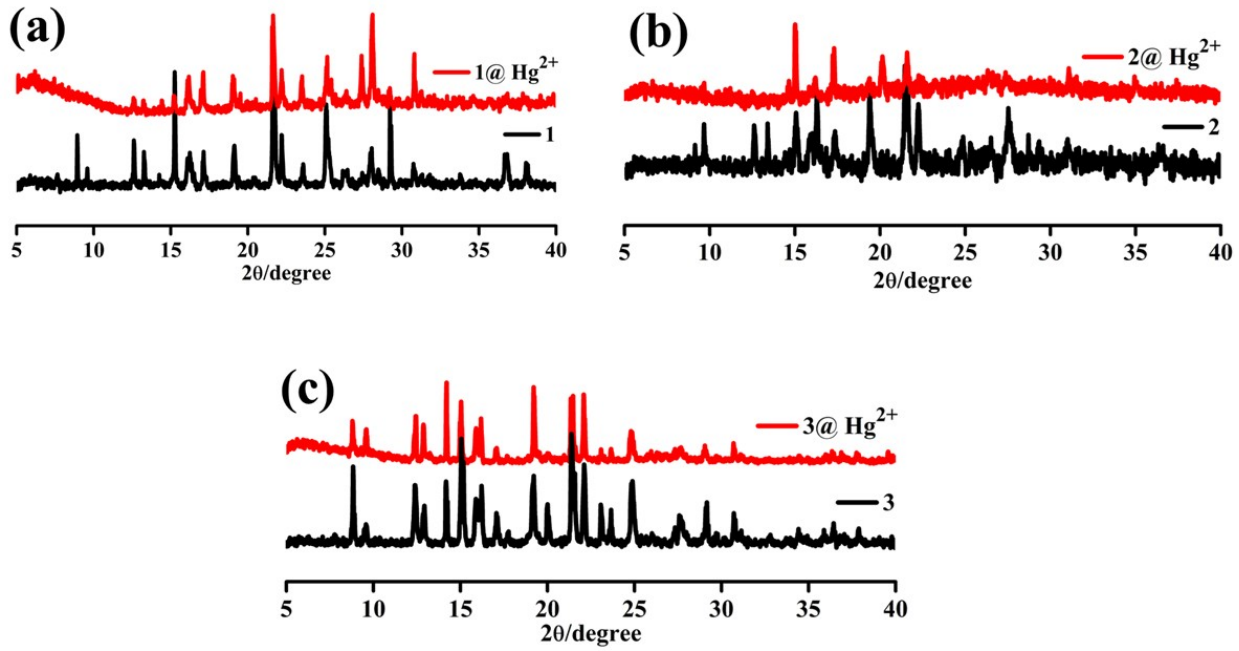

Fig. S16 PXRD peak pattern of all three compounds after treatment with 10^{-3} M aqueous Hg^{2+} solution for 5 days.

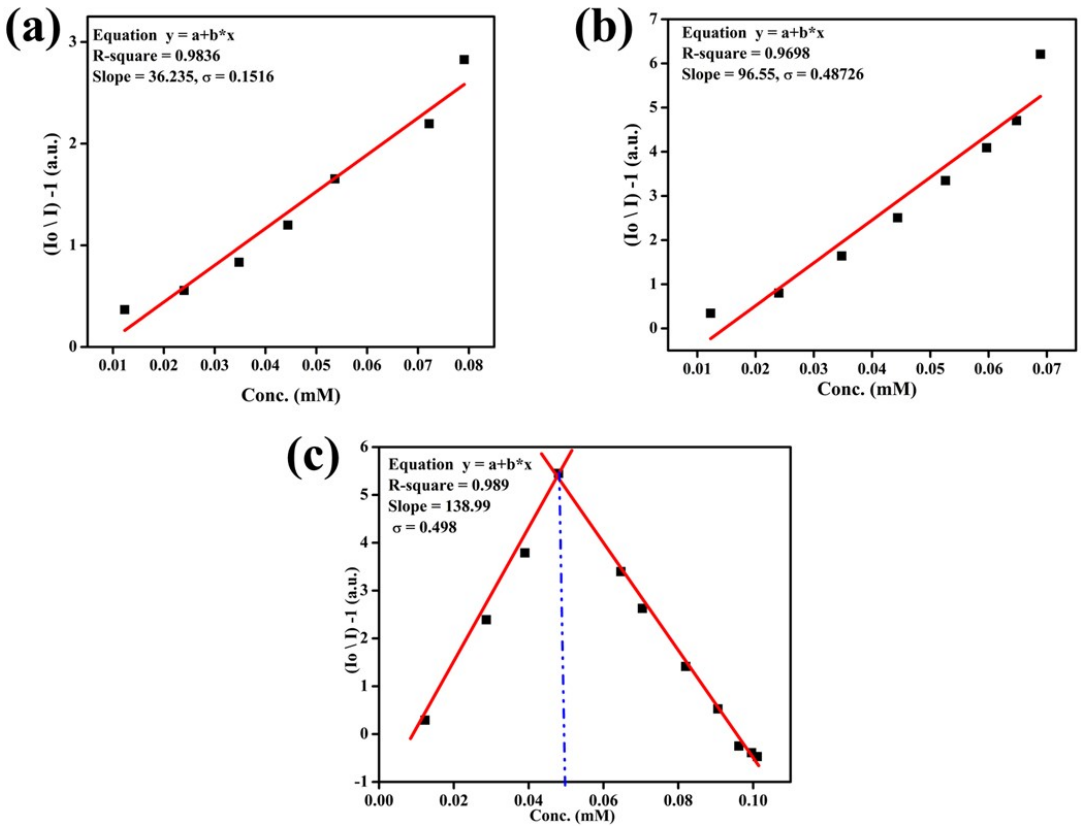

Fig. S17 (a), (b) and (c) represents linear responses of compounds varying the concentration of aqueous Hg^{2+} solutions for compound **1**, **2** and **3** respectively.

Table S14. Comparison table of sensing performance toward mercury ion for compounds 1-3 with other CP/ MOF based Hg^{2+} sensors

CP/ MOF	**LOD** (μM)	**Detection process**	**Reference**
[Zn(4-pzpt)2(H2O)]n	26.70	Quenching	**1**
{[Zn(4-pzpt)2]·CH3OH}n	34.08	Quenching	**1**
$\{[Mn_2(Bript)_2(4,4'bpy)_{.5}(DMF)]\cdot(H_2O)\}_n$	48	Quenching	**2**
[Co3(L)2(H2O)6]n	12.6	Quenching	**3**
$[Pb_2(2\text{-}NCP)_2(NH2\text{-}BDC)]_n$	6.48	Quenching	**4**
TMU-34(-2H) in Acetonitrile	6.9	Quenching	**5**
$\{[Mn(bqdc)(azo)_2(H_2O)_2]\cdot 2H_2O\}_n$ (**1**)	12.55	Quenching	This Work
$\{[Co(bqdc)(azo)_2(H_2O)_2]\cdot 2H_2O\}_n$ (**2**)	15.13	Quenching	
$\{[Mn(bqdc)(bpe)_2(H_2O)_2]\cdot 2H_2O\}_n$ (**3**)	10.74	Ratiometric	

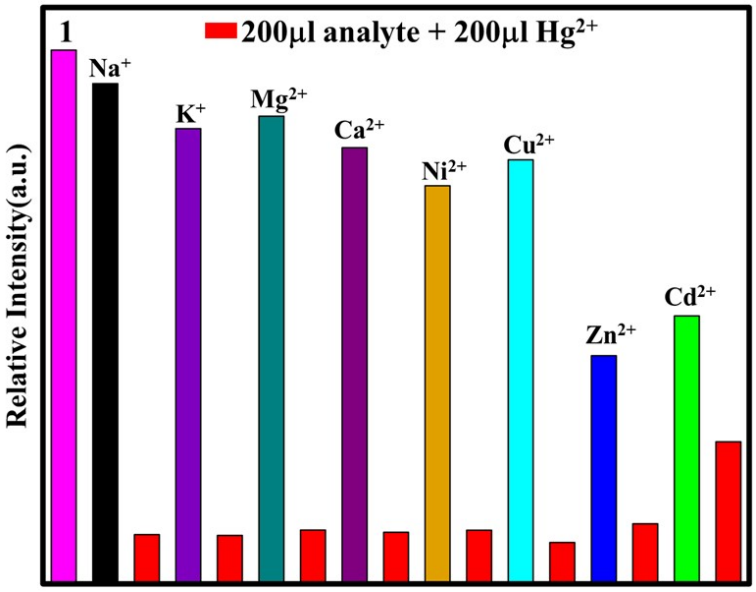

Fig. S18 Bar diagram showing the emission intensity of compound **1** in the presence of Hg^{2+} ions compared with other interfering metal ions.

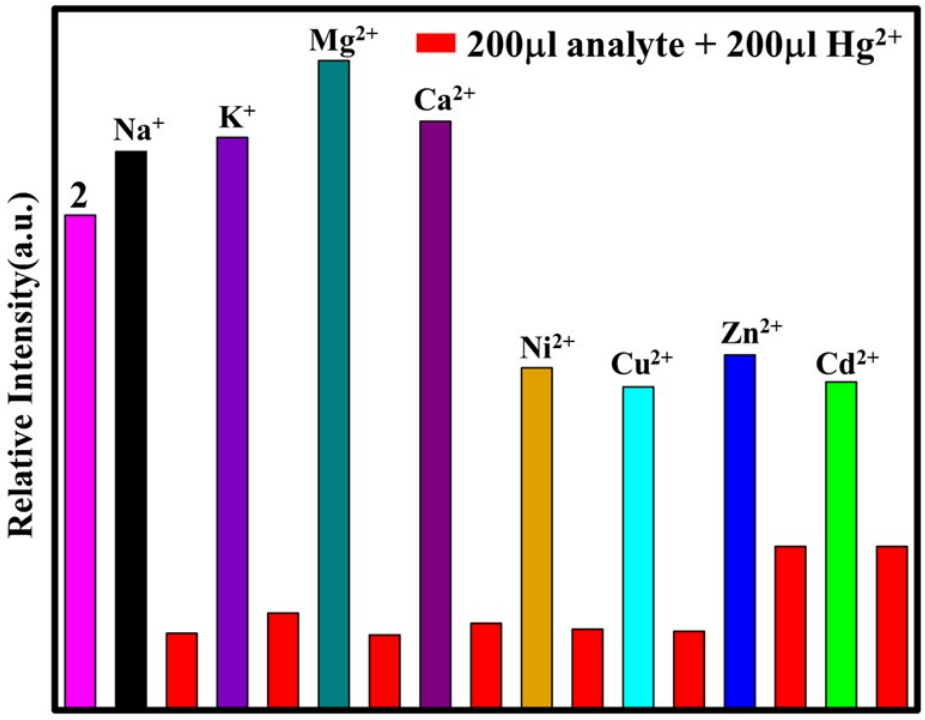

Fig. S19 Bar diagram showing the emission intensity of compound **2** in the presence of Hg^{2+} ions compared with other interfering metal ions.

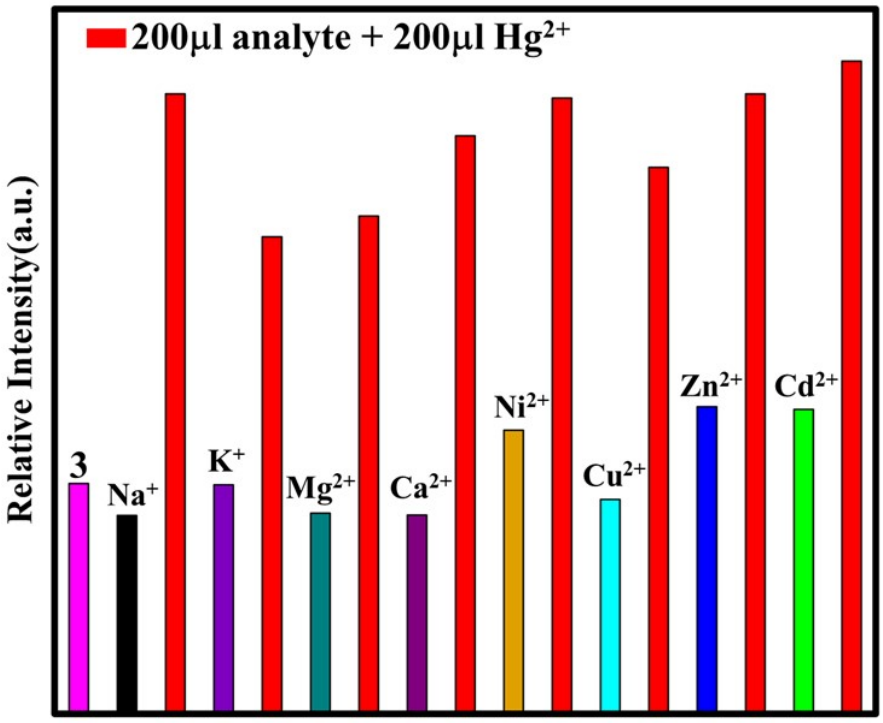

Fig. S20 Bar diagram showing the emission intensity of compound **3** in the presence of Hg^{2+} ions compared with other interfering metal ions.

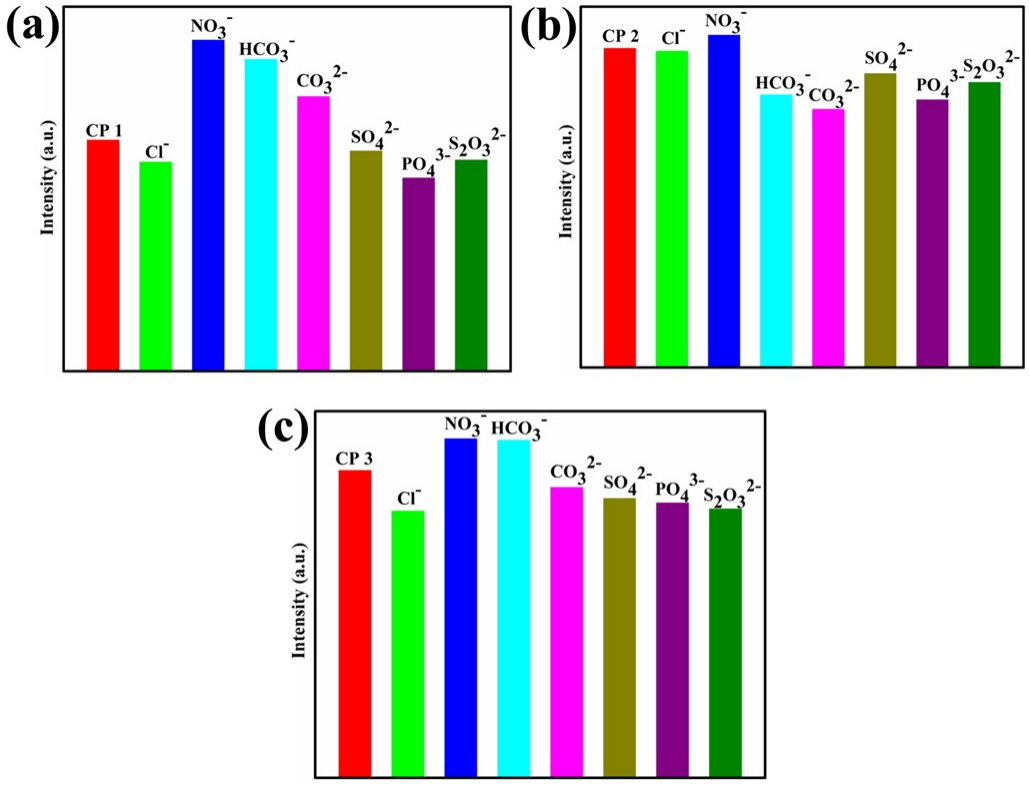

Fig. S21 Bar diagram showing the emission intensity of all three compounds in the presence of some anion.

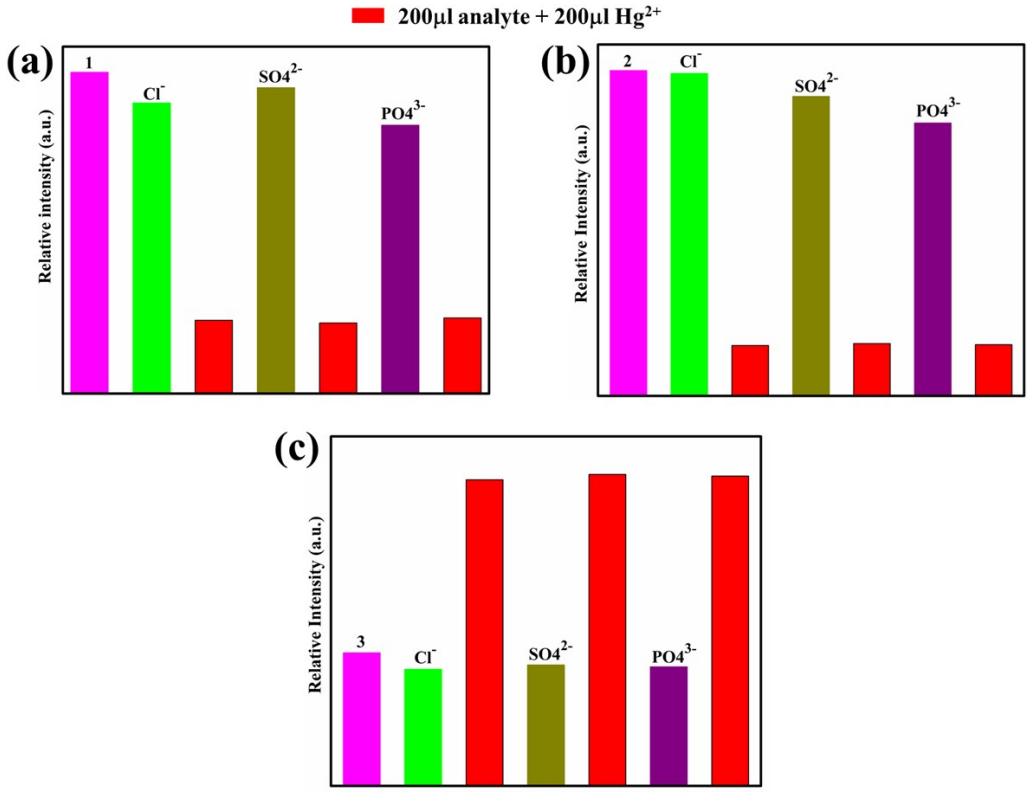

Fig. S22 Bar diagram showing the emission intensity of all three compounds in the presence of Hg^{2+} ions and some other interfering anions simultaneously.

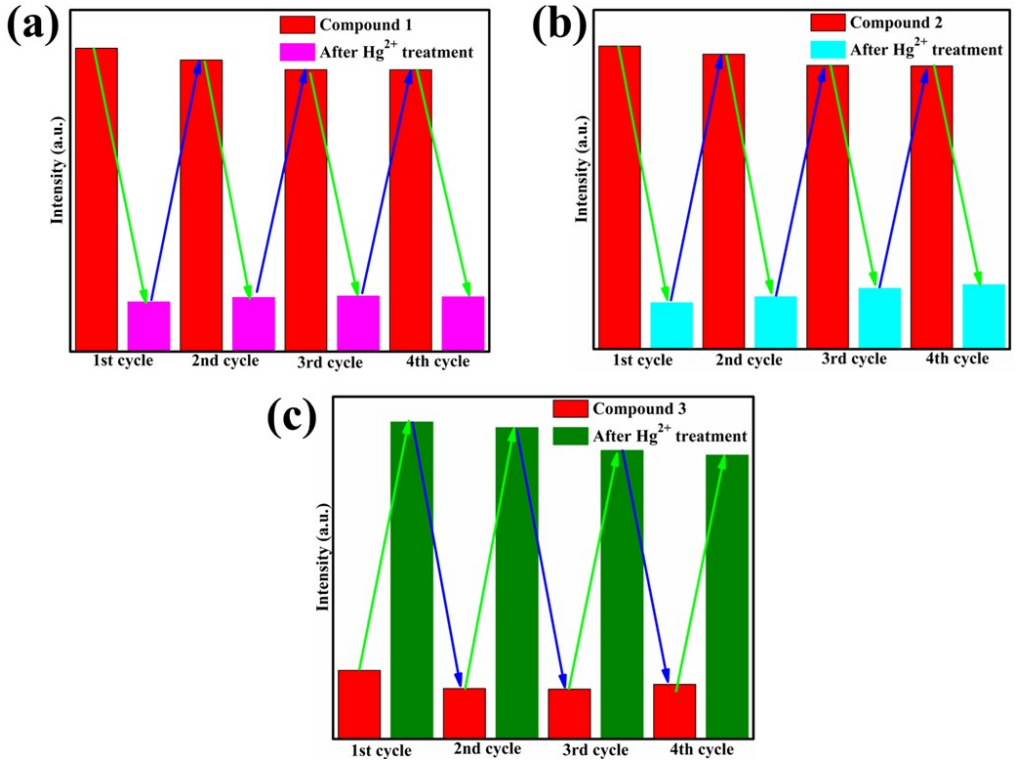

Fig. S23 Recyclability for all three compounds, each cycle is repeated with proper washing the sample.

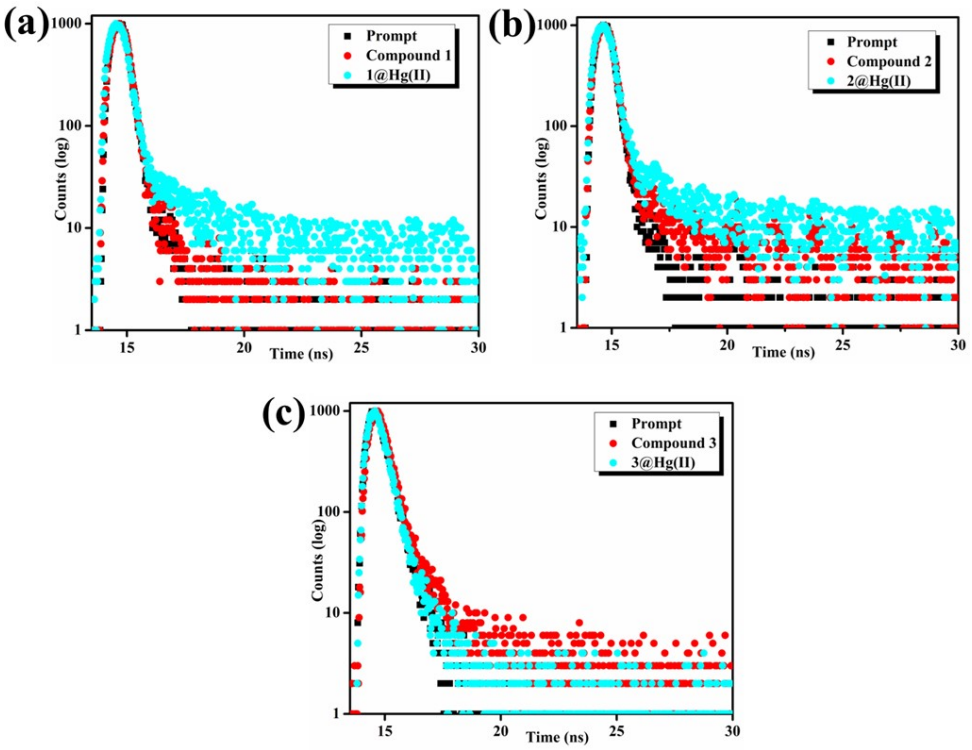

Fig. S24 Lifetime plot for all three compound (a) **1**, (b) **2** and (c) **3**

Table S15. Lifetime data for compound **1**, **2** and **3**

System	Condition	Lifetime
CP-1	**In water**	$\tau_1 = 2.20$ ns
		$\tau_2 = 1.08$ ns
	In presence of aq. Hg (II) solutions	$\tau_1 = 1.23$ ns
		$\tau_2 = 5.31$ ns
CP-2	**In water**	$\tau_1 = 1.27$ ns
		$\tau_2 = 2.54$ ns
	In presence of aq. Hg (II) solutions	$\tau_1 = 0.96$ ns
		$\tau_2 = 4.01$ ns
CP-3	**In water**	$\tau_1 = 0.34$ ns
		$\tau_2 = 1.29$ ns
	In presence of aq. Hg (II) solutions	$\tau_1 = 0.32$ ns
		$\tau_2 = 0.83$ ns

References

1. J. -X. Wang, T.-T. Wu, M. -Q. Tuo, H. -B. Pan, J. Ge, P. -P. Huang, J. -H. Gao, M. Jiang and J. -F. Lu, *Polyhedron*, 2024, **252**, 116884.
2. Y. Li, D. Ma, C. Chen, M. Chen, Z. Li, Y. Wu, S. Zhu and G. Peng, *J. Solid State Chem.*, 2019, **269**, 257-263.
3. Y. Xi, M. Hua, L. Gao, Q. Suna, E. Maa, W. Hua, M. Li, W. Liua, J. Suna and C. Zhang, *J. Mol. Struct.*2023, **1284**, 135456.
4. Y. Qiao, J. Guo, D. Li, H. Li, X. Xue, W. Jiang, G. Che and W. Guan, *J. Solid State Chem.*, 2020, **290**, 121610.
5. S. A. A. Razavi, M. Y. Masoomi and A. Morsali, *Inorg. Chem.*, 2017, **56**, 9646–9652.